JOURNAL OF OPTOELECTRONICS AND ADVANCED MATERIALS Vol. 9, No. 10, October 2007, p. 3143 - 3148

Excitation and luminescence mechanisms of Er^{3+} centers in GeGaSe chalcogenide glasses

T. AOKI*, D. SAITOU, S. KOBAYASHI, C. FUJIHASHI, K. SHIMAKAWA[a], K. KOUGHIA[b], M. MUNZAR[b], S. O. KASAP[b]

Graduate School of Electronics, Joint Research Center of High-technology, Tokyo Polytechnic University, Atsugi 243-0297, Japan

[a]*Department of Electrical and Electronic Engineering, Gifu University, Gifu 501-1193, Japan*

[b]*Department of Electrical Engineering, University of Saskatchewan, 57 Campus Drive, Saskatoon, SK, S7N 5A9, Canada*

Wideband quadrature frequency resolved spectroscopy (QFRS) of photoluminescence (PL) from 2 ns to 160 s reveals significantly different lifetime distributions between undoped and Er-doped GeGaSe chalcogenide glasses (ChGs). The QFRS of the undoped GeGaSe ChGs exhibits a triple-peak lifetime distribution. The two short-time peaks are associated with the singlet-triplet excitons, and the third peak, at much longer lifetimes, $\tau_H \approx 20$ s, is associated with radiative tunneling recombination at low temperatures, similar to other amorphous semiconductors. The QFRS of the Er-doped GeGaSe ChGs exhibits a double-peak lifetime distribution, consisting of a peak at $\tau_{Er} \approx 3$ ms, a characteristic of the Er^{3+} luminescent center, and another peak at $\tau_H \approx 20$ s, even at room temperature. We report detailed QFRS measurements as a function of temperature T, PL emission energy $\hbar\omega$ and PL excitation energy E_X, and discuss the results in terms of possible mechanisms for the origin of the individual lifetime components for the undoped and Er-doped GeGaSe ChGs.

(Received July 3, 2007; accepted October 1, 2007)

Keywords: PL, QFRS, Lifetime, Slow luminescence, Thermal quenching

1. Introduction

Chalcogenide glasses are known to be promising materials for applications in telecommunications and integrated photonics because they are transparent over a wide range of wavelengths in the infrared region, and possess high refractive indices and low phonon energies. Moreover, GeGaSe clalcogenide glasses (ChGs) in particular have been shown to be excellent Er-host materials since they allow homogeneous Er-doping in large amounts (e.g. up to 2 at.% Er) with the subsequent formation of Er^{3+} ions [1]. The photoluminescence (PL) of *f-f* transitions ($^4I_{13/2} \rightarrow {}^4I_{15/2}$) in Er^{3+} centers in Er-doped GeGaSe ChGs with a near-stoichiometric composition and a high concentration of Ga features a single dominant peak in the PL spectrum at ~1.5 μm with a typical PL lifetime $\tau_{Er} \approx 3$ ms, which is almost independent of temperature T, and whose exact value is only slightly affected by the exact composition of the host GeGaSe ChGs. The relatively long lifetime of ~3 ms and the ability to dissolve high concentrations of Er^{3+} make this Er-doped ChGs a potential candidate material for applications in optical amplifiers and lasers [2].

However, the PL mechanisms in these materials are still far from being understood and require further investigation for the excitation and de-excitation of the Er^{3+} luminescence centers in the Er-doped GeGaSe ChGs [3-5]. Moreover, in order to more comprehensively understand the PL mechanisms of the Er^{3+} center, a detailed investigation of PL in the undoped GeGaSe ChGs host is needed. Quadrature frequency resolved spectroscopy (QFRS) yields detailed information on widespread lifetime distributions in amorphous semiconductors compared with a conventional PL decay measurement. On measuring the PL decay with multi-lifetime components, one must decrease the photocarrier generation rate G sufficiently to avoid the occurrence of nonlinearities, and to ensure a geminate recombination condition, because a short-lived component appears in the decay immediately after the cessation of PL excitation. However, sometimes a long-lived component decreases to an undetectable level at the time corresponding to its own lifetime in the PL decay. On the other hand, the QFRS can discriminate a small lifetime component against the main lifetime component with sufficient sensitivity by virtue of the dual lock-in detection techniques used in this measurements system [6].

In our previous works, a wideband QFRS from 2 ns to 160 s revealed a new PL component peaked at a slow lifetime $\tau_H \approx 16$ s at temperatures 3.7 and 294 K (room temperature) in addition to the main Er^{3+} emission peak at $\tau_{Er} \approx 3$ ms in the Er-doped GeGaSe ChGs [7]. The slow τ_H-component consists of two PL peaks at the PL emission energies $\hbar\omega \approx 0.81$ and 1.27 eV corresponding to the $^4I_{13/2} \rightarrow {}^4I_{15/2}$ and $^4I_{11/2} \rightarrow {}^4I_{15/2}$ transitions, respectively, in spite of its lifetime τ_H being much longer than τ_{Er} intrinsic to the Er^{3+} luminescence center. On the other hand, the QFRS spectrum of the undoped GeGaSe ChGs has three peaks at 3.7 K. The first two peaks at

~20 ns and ~90 μs are ascribed to singlet and triplet excitons respectively. There is a third slow peak at τ_H ≈16 s, as observed in the Er-doped sample.

The very small dependence of the τ_H-component on G and PL excitation energy E_X in both the doped and undoped samples and the IR-induced quenching of the τ_H component suggest a type of slow emission that is related to the radiative tunneling between tail-trapped photocarriers (after their hopping in the tail states) and D^0 centers competing with a non-radiative tunneling to defects and impurity states [7,8]. Reflecting on these experimental results, we invoked the defect-related Auger effect (DRAE) to interpret the energy transfer from precursors to the Er^{3+} centers in both the τ_{Er}- and τ_H-components [9].

Continuing from the previous works, the present paper presents the results of PL lifetime distributions from 2 ns to 160 s in undoped and Er-doped GeGaSe ChGs from wideband QFRS. In particular, we report the PL emission energy $\hbar\omega$, temperature T and excitation energy E_X dependences of the lifetime distribution, and discuss the excitation and luminescence mechanisms of the Er^{3+} centers.

2. Experimental

Er-doped GeGaSe ChGs of the actual composition $Ge_{28}Ga_6Se_{64.7}S_{0.8}Er_{0.5}$, which has been doped with Er_2S_3, and undoped ChGs of the actual composition $Ge_{27}Ga_9Se_{64}$ were synthesized by mixing and melting in fused silica ampoules in a rocking furnace at 980 °C for 24 h and then quenching the ampoules in water. The density of Er^{3+} center is estimated at ~5×10^{19} cm^{-3} for the 0.5 % Er-doped sample. The thickness was ~1.2 mm for the undoped sample and ~2.4 mm for the Er-doped one. The samples were excited by various lasers operating at E_X = 1.27, 1.58, 1.70, 1.81, 1.94, 2.33 and 3.04 eV, and PL was detected by a Hamamatsu 5509-72 infrared photomultiplier (PMT) at the photon energy of ~0.73 eV (~1.7 μm) or greater with a long-pass filter to cut off the PL excitation light. Occasionally the PL was dispersed by a 10 cm-f/3.0 monochromator with a resolution of ~30 meV, which was installed between sample and PMT.

The PL lifetime distributions were measured by a wideband QFRS system from 2 ns to 160 s, consisting of DPDL (dual-phase double-lock-in) and internal lock-in methods [6]. The optical absorption spectra and absorption coefficients were obtained by fiber-optic transmission measurements using a Perkin-Elmer Lambda 900 spectrometer at 3.7 K. The sample temperature was controlled between 3.7 and 300 K using a closed-cycle He cryostat.

3. Results and discussions

Fig. 1(a) shows QFRS spectra for various monochromatized PL emission energies $\hbar\omega$, i.e., $\hbar\omega$-evolved QFRS spectra at $T \approx 3.7$ K and $E_X = 2.33$ eV with $G \approx 10^{20}$ $cm^{-3}s^{-1}$. The observed spectra are triple-peaked. The peaks at τ_S and τ_T are the well-known double peaks observed in a-Si:H and various amorphous semiconductors [10-13], and third peak located around at a lifetime $\tau_H \approx 20$ s was previously reported by our group [7]. The quantum efficiencies (QEs) η_S, η_T and η_H corresponding to the τ_S-, τ_T- and τ_H-components obtained by deconvoluting the $\hbar\omega$-evolved QFRS spectra are plotted as functions of $\hbar\omega$, i.e. the PL spectra of the individual recombination components in Fig. 1(b). The peak energy of the τ_S-component at ~1.02 eV is higher by ~80 meV than that of the τ_T-component that peaks at ~0.94 eV, from which the spectrum of the slow τ_H-component does not differ too much. Fig. 1(c) shows the recombination rate ($1/\tau$) of each component as a function of $\hbar\omega$ on a log-log scale. The recombination rates τ_S^{-1} and τ_T^{-1} roughly depend on $\hbar\omega$ as $(\hbar\omega)^3$, suggesting that the τ_S- and τ_T-components are ascribed to the excitonic recombination process [14]. On the other hand, the recombination rate τ_H^{-1} is independent of $\hbar\omega$, which suggests that it should be ascribed to radiative tunneling recombination of photoexicted carriers after hopping down in tail-states, in spite of the very small dependence of τ_H on G and E_X [7, 14].

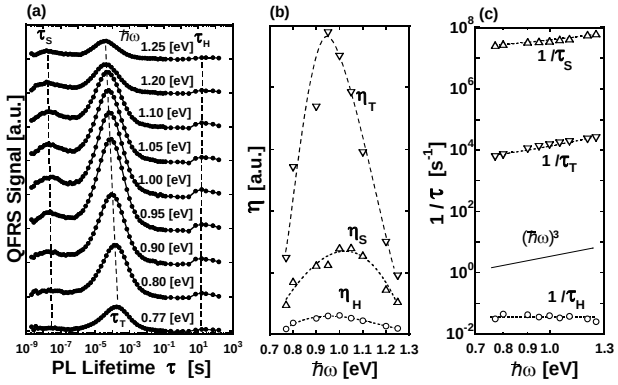

Fig. 1. (a) PL emission energy ħω-evolved QFRS spectra of the undoped GeGaSe sample at the PL excitation energy E_X = 2.33.eV, the temperature T = 3.7 K and the genration rate $G \approx 10^{20}$ $cm^{-3}s^{-1}$. (b) The three componets of (Δ) τ_S, (▽) τ_T and (○) τ_H deconvoluted from (a) as functions of ħω, i.e., PL spectra of QEs η_S, η_T and η_H. (c) radiative recombination rates ($1/\tau$) of the three components (Δ) τ_S, (▽) τ_T and (○) τ_H plotted against ħω on a log-log scale.

The formation of the three lifetime components are interpreted on the basis of the Mott-Davis-Street (MDS) model [15], The bound singlet- and triplet-excitons consist of a free electron and a hole trapped at D^0 center, or a free hole and an electron trapped at a D^0 center, and the slow τ_H-component recombination occurs between a carrier localized at a tail-state, after down-hopping, and an oppositely charged carrier trapped at a D^0 center [7].

Fig. 2(a) shows T-evolved QFRS spectra of the undoped sample, where each spectrum is normalized by the total PL intensity obtained from the PMT DC current. A rise in T increases the τ_S-component in comparison with the τ_T-component. In Fig. 2(b), the relative QE of the τ_S- to τ_T-components is plotted against $10^3/T$,

showing an activation energy $E_a \approx 78$ meV at higher T. This coincides with the PL peak-energy difference of ~80 meV between the τ_S- and τ_T-components in Fig. 1(b), which also supports that the τ_S- and τ_T-components are attributed to singlet- and triplet-excitons, respectively, with a spin-exchange energy of ~80 meV. The third component of the lifetime τ_H is quenched at room temperature in the undoped sample.

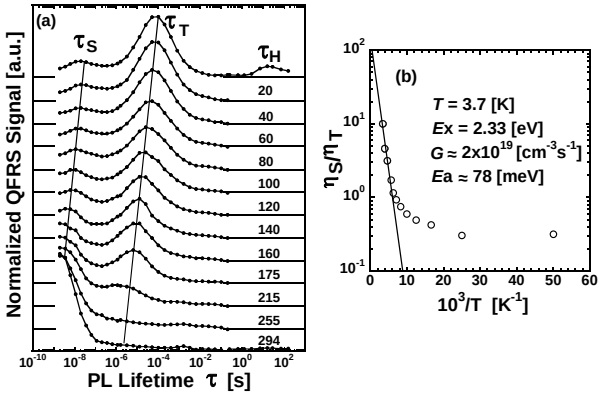

Fig. 2. (a) Temperature T-evolved QFRS spectra of the undoped GeGaSe sample at E_X = 2.33.eV and $G \approx 10^{19}$ $cm^{-3}s^{-1}$. (b) Ratio of QEs of two excitonic components η_S/η_T as a function of the inverse of temperature $10^3/T$, where QEs η_S and η_T are deconvoluted from (a).

By deconvoluting the T-evolved QFRS spectra of Fig. 2(a), the QEs η_S and η_T of the corresponding τ_S- and τ_T-components are plotted as functions of T in addition to the lifetimes τ_S and τ_T in Fig. 3. Generally the QE η is reduced by non-competing NRR and/or competing NRR in amorphous semiconductors. The non-competing NRR is introduced by defects and impurities, which rapidly capture photoexcited carriers normally within 10^{-12} s during the thermalization of photocarriers from extended or higher tail states after the PL excitation. The non-competing NRR reduces η without shortening the measured PL lifetime τ. On the other hand, the competing NRR with a lifetime τ_{nr} competes with the radiative recombination with a lifetime τ_r and the measured or effective lifetime τ is given by

$$\tau^{-1} = \tau_r^{-1} + \tau_{nr}^{-1}, \qquad (1)$$

and the QE η is expressed as,

$$\eta = \eta_{nc} \frac{\tau_r^{-1}}{\tau_r^{-1} + \tau_{nr}^{-1}} = \eta_{nc} \frac{\tau}{\tau_r} \quad , \qquad (2)$$

where η_{nc} is a QE subject to the non-competing NRR and τ/τ_r is a QE subject to the competing NRR. The competing NRR lifetime τ_{nr} shortens with increasing T, whereas τ_r is usually independent of T. Hence the T-dependence of the QE, τ/τ_r, is proportional to that of the measured lifetime τ.

In Fig. 3, however, the decreases of the QEs η_S and η_T with increasing T are much more than those of the lifetimes τ_S and τ_T. The difference is due to the contribution of η_{nc} to the decrease in both η_S and η_T. Thus, the non-competing NRR plays a significant part in the thermal quenching of the excitons; namely as T rises from 3.7 to 294 K, η_{nc} decreases by about two orders of magnitude for the τ_S-component and by three orders of magnitude for the τ_T-component. The QEs, τ/τ_r, of τ_S- and τ_T-components show a similar T-dependence as $\exp(-T/T_0)$ with $T_0 \approx 53$ K estimated from the dotted lines in Fig. 3, and thus the characteristic temperature $T_0 \approx 53$ K for the competing NRR of both the τ_S- and τ_T-components.

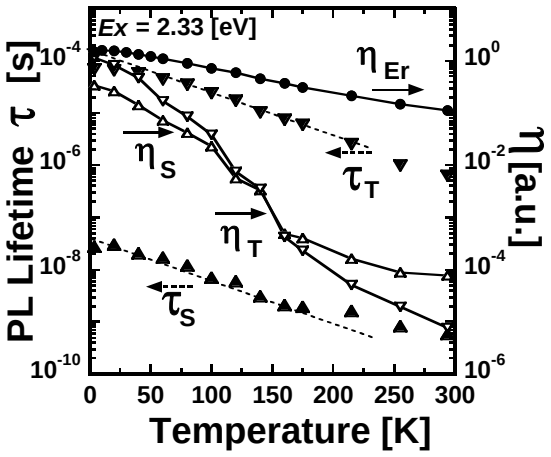

Fig. 3. QEs (Δ) η_S, (▽) η_T and lifetimes (▲) τ_S, (▼) τ_T of the two excitonic components as funcruions of T obtained from Fig. 2(a) of the undoped GeGaSe ChGs. (●) QE η_{Er} of the τ_{Er} component of the Er-doped sample is also plotted.

Among several theoretical derivations for T_0 [16-18], the following expression may be appropriate for the two excitonic components,

$$T_0 = \varepsilon_0 k^{-1} \ln^{-1}\left(\nu_0 \tau_r \frac{N_{nr}}{N_{nr} + N_r} \right), \qquad (3)$$

with a characteristic energy of localized states ε_0, the Boltzmann constant k, the attempt-to-escape constant ν_0, normally ~10^{12} s^{-1}, the concentration of competing NRR centers N_{nr} and the concentration of radiative states N_r [18]. T_0 being identical for both the τ_S and τ_T components in spite of the difference of τ_r at the low $T \approx 3.7$ K, i.e. $\tau_r = \tau_S \approx 20$ ns and $\tau_r = \tau_T \approx 90$ μs suggests the invariance of the term in the parenthesis of the eq. (3).

The asymptotic ratio of the QE τ/τ_r at a sufficiently high T to that at T = 0 is theoretically expressed as

$[1+\nu_0\tau_r N_{nr}/(N_{nr}+N_r)]^{-1}$ [18]. Since it amounts to $\sim 10^{-2}$ in Fig. 3 for both the lifetimes τ_S and τ_T, the term $N_{nr}/(N_{nr}+N_r)$ must be modified by weighing N_{nr} and N_r with the corresponding capture cross sections; the capture cross section for N_{nr} of the triplet exciton is, therefore, smaller by a factor of $\sim 2\times 10^{-4}$ than that of the singlet exciton, probably due to the spin-selection rule. We then obtain a plausible value of $\varepsilon_0 \approx 20$ meV for the two recombination components.

The observations are distinctly different for the Er-doped GeGaSe sample. It is shown in the Fig. 3 that the QE η_{Er} of the τ_{Er}-component, i.e. the $^4I_{13/2} \rightarrow {}^4I_{15/2}$ emission decreases only by an order of magnitude for a T increase from 3.7 to 294 K at E_X = 2.33 eV, while the lifetime $\tau_{Er} \approx 3.4$ ms remains the same as shown in Fig. 4. This suggests the absence of a competing NRR that would modify τ_{Er} through eq. (1). The τ_{Er}-component is thus quenched by the non-competing NRR through η_{nc} in eq. (2). As T rises from 3.7 to 294 K, η_{nc} of the τ_{Er}-component decreases only by one order of magnitude, whereas η_{nc} of the τ_S- and τ_T-components decrease by nearly two and three orders of magnitude, respectively, in the undoped ChGs.

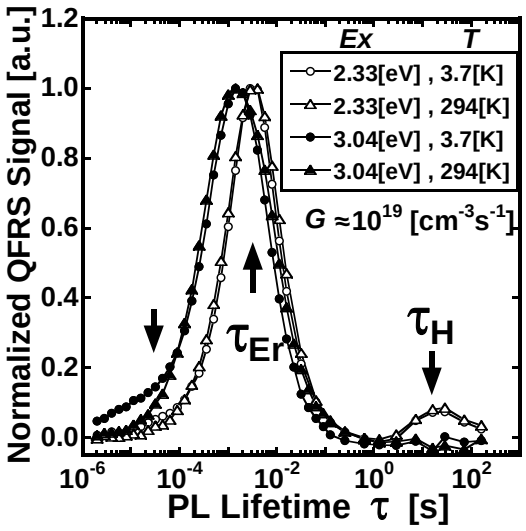

Fig. 4. QFRS spectra of the Er-doped GeGaSe sample at $G \approx 10^{19}$ $cm^{-3}s^{-1}$ for two different PL excitation energies E_X and temperatures T. (○) E_X = 2.33.eV and temperature T = 3.7 K, and (Δ) E_X = 2.33.eV but T = 294 K. (●) E_X = 3.04 eV and T = 3.7 K, and (▲) E_X = 3.04 eV but T = 294 K.

In the Er-doped sample, the slow component with $\tau_H \approx 20$ s is still observable at T = 294 K and E_X = 2.33 eV without any changes in the QFRS spectrum at T = 3.7 K, except for the magnitude (Fig. 4); the competing NRR is completely absent even in the slow τ_H-emission process as well as the $^4I_{13/2} \rightarrow {}^4I_{15/2}$ emission of the τ_{Er}-component. This implies that the Er^{3+} luminescent center in GeGaSe ChGs is extremely isolated from the competing NRR and possesses no back-transfer process [19].

On exciting the sample at E_X = 3.04 eV far above-bandgap with $G \approx 10^{19}$cm^{-3}s^{-1}, no τ_H-component can be seen at both the low and high Ts (Fig. 4); the magnitude of the τ_{Er} component is also reduced at E_X = 3.04 eV. The photoexcited carriers are more concentrated close to an illuminated surface due to a large absorption coefficient at the high E_X and diffuse to the surface with subsequent surface NRR. This surface NRR competes with the volume recombination. The ratio of surface-to-volume recombination is proportional to $S(\tau/D)^{1/2}$, where S is the surface recombination velocity and D is the diffusion constant of the carriers [20]. Thus the τ_H-component is quenched by a high $S(\tau/D)^{1/2}$ with the long lifetime $\tau = \tau_H$ and the low D of the localized carriers.

As shown in Fig. 4, the measured lifetime of the main Er^{3+} emission at $\tau = \tau_{Er}$ is ~1.6 ms at E_X = 3.04 eV in contrast to $\tau_{Er} \approx 3.4$ ms at E_X = 2.33 eV. Moreover, at E_X = 1.27 eV (980 nm) corresponding to $^4I_{15/2} \rightarrow {}^4I_{11/2}$ excitation of the Er^{3+} center at T = 3.7 K and $G \approx 10^{16}$cm^{-3}s^{-1}, τ_{Er} is ~5.0 ms as shown in Fig. 5, along with the QFRS spectra at E_X =2.33 and 3.04 eV. The contradiction $\tau > \tau_r$ in eq. (1) between the measured lifetime τ_{Er} and the radiative transition time $\tau_r \approx 1.8$ ms for the $^4I_{13/2} \rightarrow {}^4I_{15/2}$ manifolds determined by the Judd-Ofelt analysis was interpreted in terms of multiple radiation reabsorption and re-emission processes, i.e. energy transfer via reabsorption and re-emission at Er^{3+} luminescence centers [21, 22]. (The latter model was able to explain the differences in τ between the front- and back-side PL excitations.) A little shorter lifetime $\tau_{Er} \approx 1.6$ ms at E_X = 3.04 eV than the Judd-Ofelt lifetime $\tau_r \approx 1.8$ ms is probably attributed to the competing surface-NRR [20].

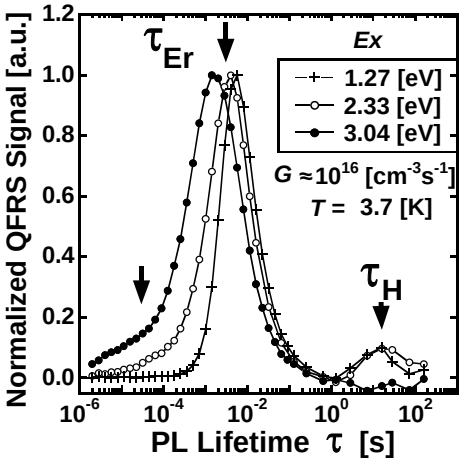

Fig. 5. QFRS spectra of the Er-doped GeGaSe sample for three different PL excitation energies E_X at T = 3.7 K with $G \approx 10^{16}$ $cm^{-3}s^{-1}$. (+) E_X = 1.27eV (980 nm) corresponding to the $^4I_{15/2} \rightarrow {}^4I_{11/2}$ transition, (○) E_X = 2.33.eV and (●) E_X = 3.04 eV.

Fig. 6 shows the QFRS spectra of the undoped GeGaSe ChGs for various E_X from sub-bandgap excitation of 1.58 eV to the above-bandgap excitation of 3.04 eV, where the QFRS signals, normalized by the PL excitation power, are plotted on a log-log scale. The three components vary significantly with E_X. As E_X decreases below the Tauc-bandgap energy of ~1.9 eV at 3.7 K, the QFRS spectra in the τ_S and τ_S regions become almost featureless and, at the same time, the τ_H-component becomes large compared with other components. At the sub-bandgap excitation, the τ_H-component may be formed by direct excitation of an electron at a D^- center to a deep tail-state of the conduction band or by its complementary process, i.e. the excitation of an electron at a deep tail state of valence band to D^+ center [7]. This is also the case for the Er-doped sample in Fig. 5, where the τ_H-component exists even at the sub-bandgap excitation of E_X = 1.27 eV.

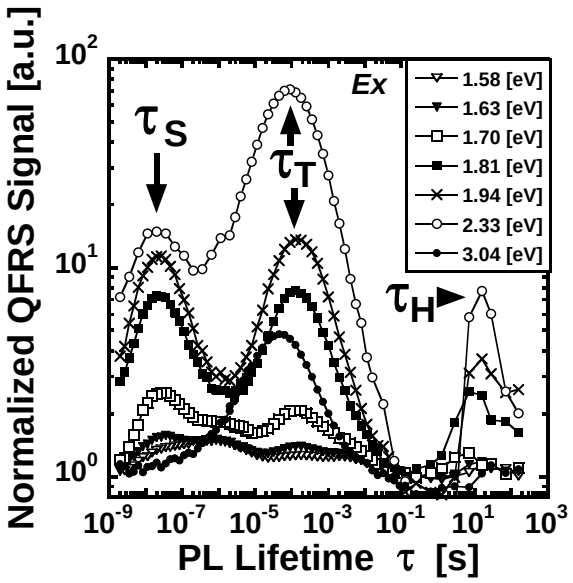

Fig. 6. QFRS spectra of the undoped GeGaSe sample at T = 3.7 K and G ≈ 10^{17} $cm^{-3}s^{-1}$ for various PL excitation energies E_X; (▽) 1.58 eV, (▼) 1.63 eV, (□) 1.70 eV, (■) 1.81 eV, (×) 1.94 eV, (○) 2.33 eV, (●) 3.04 eV.

Moreover, Fig. 6 shows that the ratio of the τ_T- to τ_S-component increases as E_X increases, suggesting spin-flipping from singlet to triplet states during the thermalization of excited carriers. A subtle lifetime shortening of τ_T and disappearance of the slow component with increasing E_X are probably attributed to the competing surface NRR as mentioned above for Figs. 4 and 5. Downward arrows around at ~3×10^{-5} s in Figs. 4 and 5 indicate the background spectra of the precursor, i.e. triplet exciton for the τ_{Er}-component at low T and high E_X, where the τ_T-component is enhanced compared with the other components in Fig. 2(a) and Fig.6.

It is postulated that nearly half of the whole excitonic component of the host is converted to the τ_{Er}-component and also half of the τ_H-component of the host is converted to the slow τ_H-component of the Er-doped sample at T = 3.7 K, and that the energy transfer mechanisms for both the τ_{Er}- and τ_H-components are ascribed to the DRAE at low temperatures [7]. The PL peak energy ~0.94 eV of both the triplet exciton and the τ_H-component in the host being close to 0.81 eV of the $^4I_{13/2} \rightarrow {}^4I_{15/2}$ transition supports that those are precursors for the τ_{Er}-component and the τ_H-component of the Er-related emission, respectively, at low temperatures.

However, both the components of the Er-related emission decrease only by an order of magnitude as T rises from 3.7 K to 294 K, in contrast to the steep PL quenching of the host. Thus we cannot simply assign the precursor for the τ_{Er}-component to excitons and the precursor for the τ_H-component to a composite of a tail-trapped carrier bound to an oppositely charged carrier trapped at a D^0 center at room temperature. The reason is that since an excited precursor relaxes by transferring its energy non-radiatively to an Er^{3+} luminescence center, with the subsequent Er-emission of intrinsic lifetime $\tau_{Er} << \tau_H$, the precursor for the τ_H-component, in particular, should survive for a long time (τ_H) even at room temperature [7].

Although further investigation needs to be carried out, the DRAE is one of the promising mechanisms we can use to interpret the weak thermal quenching of PL in Er-doped GeGaSe ChGs by the high activation energy for multi-phonon relaxation as well as the low phonon energies of the GeGaSe ChGs [9]. Furthermore, the density of Er^{3+} centers amounts to ~5×10^{19} cm^{-3} for the 0.5 % Er-doped sample, which is probably larger than that of defect and impurity states including the D-states. Hence this opens a possibility of hybridizing these states with an electronic state of Er^{3+}center, e.g. the 5*d*-state, and forming stable Er-related states for the precursors against the NRR processes such as the multi-phonon relaxation even at elevated temperatures [23].

4. Summary and conclusions

PL of undoped GeGaSe ChGs (host) consists of two excitonic components with the spin-exchange energy of ~80 meV and a slow lifetime component with a lifetime $\tau_H \approx$ 20 s at T = 3.7 K. Both the singlet-exciton with a PL peak energy ~1.02 eV and a lifetime $\tau_S \approx$ 20 ns and the triplet-exciton with ~0.94 eV and $\tau_T \approx$ 90 μs can be considered as precursors for the main Er^{3+} emission with a lifetime $\tau_{Er} \approx$ 3 ms in Er-doped GeGaSe ChGs at low temperatures. However the PL quenching accompanying the temperature rise from 3.7 K to 294 K is strikingly different between the two excitonic emissions and the main Er^{3+} emission. The excitonic components of the host suffer the competing non-radiative recombination

(NRR) with an identical characteristic temperature $T_0 \approx$ 53 K, and also suffer the non-competing NRR; the latter more strongly. On the other hand, the main Er^{3+} emission of the Er-doped sample is not only independent of the competing NRR but also less dependent on the non-competing NRR. This is also the case for the slow τ_H-component; on raising T to 294 K, the slow component of the host disappears but that of the Er-doped sample continues to exist, suggesting that its precursor is able to survive for a long time $\sim\tau_H$ even at room temperature.

Decreasing the excitation energy E_X for the Er-doped sample from 3.04 eV to 1.27 eV corresponding to the $^4I_{15/2} \rightarrow {}^4I_{11/2}$ excitation of Er^{3+} center at T = 3.7 K extends the lifetime τ_{Er} from ~1.6 ms to ~5.0 ms, as interpreted earlier using the reabsorption and re-emission model. At an above-band gap excitation of E_X = 3.04 eV, the slow component in the Er-doped sample as well as the host is absent even at the lowest T = 3.7 K due to the competing surface NRR. On the contrary, at a sub-band gap excitation of E_X = 1.27 eV, the slow τ_H-component is still found and the relative enhancement of the slow component is observed at the sub-bandgap excitation of the host. This suggests the direct excitation of a carrier from D^- or D^+ center to a deep tail-state.

The DRAE model looks highly promising for interpreting the results presented, though the precursors for the main Er^{3+} emission, i.e. the τ_{Er}-component as well as the slow τ_H-component should be further investigated at higher temperatures. Moreover, it is suggested that Er-related states are induced in the precursors by the high concentration of Er-ions and stabilize PL in the Er-center against thermal quenching.

Acknowledgements

The work was financially supported in part by the Japan Private School Promotion Foundation.

References

[1] M. Munzar, K. Koughia, T. Tonchev, K. Maeda, T. Ikari, C. Haugen, R. Decorby, J. N. McMullin, S. O. Kasap, Opt. Mater. **28,** 225 (2005).
[2] K. Koughia, D. Saitou, T. Aoki, M. Munzar, S. O. Kasap, J. Non-Cryst. Solids **352**, 2420 (2005).
[3] W. Fuhs, I. Ulber, G. Weiser, M. S. Bresler, O. B. Gusev, A. N. Kuznetsov. V. Kh. Kudoyarova, E. I. Terukov, I. N. Yassievich, Phys. Rev. B **56**, 9545 (1997).
[4] H. Kühne, G. Weiser, E. I. Terukov, A. N. Kuznetsov, V. Kh. Kudoyarova, J. Appl. Phys. **86**, 896 (1999).
[5] S. G. Bishop, D. A. Turnbull, B. G. Aitken, J. Non-Cryst. Solids, **266**-**269**, 876 (2000).
[6] T. Aoki, Optical Properties of Condensed Matter and Applications, ed. By J.Singh, John Wiley & Sons, Chichester (2006) p.75.
[7] T. Aoki, D. Saitou, S. Kobayashi, C. Fujihashi, K. Shimakawa, M. Munzar, K. Koughia, S. O. Kasap, J. Mater Sci: Mater Electron. **18,** 000 (2007) [in press].
[8] T. Aoki, K. Ikeda, N. Ohrui, S. Kobayashi, K. Shimakawa, J. Optoelectron. Adv. Mater. **9**, 70 (2007).
[9] I. Yassievich, M. Bresler, O. Gusev, J. Non-Cryst. Solids, **226**, 192 (1998).
[10] F. Boulitrop, D. J. Dunstan, J. Non-Cryst. Solids **77**-**78**, 663 (1985).
[11] T. Aoki, J. Non-Cryst. Solids **352**, 1138 (2006).
[12] T. Aoki, S. Komedoori, S. Kobayashi, T. Shimizu, A. Ganjoo, K. Shimakawa, J. Non-Cryst. Solids **326**-**327**, 273 (2003).
[13] T. Aoki, D. Saito, K. Ikeda, S. Kobayashi, K. Shimakawa, J. Optoelectron. Adv. Mater. **7**, 1749 (2005).
[14] T. Aoki, K. Ikeda, S. Kobayashi, K. Shimakawa, Philos. Mag. Lett. **86**, 137 (2006).
[15] E. Davis, Amorphous Semiconductors, ed. By M. H. Brodsky, Springer-Verlag, Berlin (1979) p.41.
[16] C. M. Gee, M. Kastner, Phys. Rev. Lett. **42**, 1765 (1979)
[17] R. A. Street, Hydrogenated amorphous silicon, Cambridge University Press, Cambridge (1991) p. 302.
[18] O. Rubel, S. D. Baranovskii, K. Hantke, B. Kunert, W. W. Rühle, P. T. Thomas, K. Volz, W. Stolz, Phys. Rev. B **73**, 233201 (2006).
[19] P. G. Kik, M. J. A. de Dood, K. Kikoin, A. Polman, Appl. Phys. Lett. **70**, 1721 (1997).
[20] S. G. Bishop, D. L. Mitchell, Phys. Rev. B **8**, 5696 (1973).
[21] K. Koughia, M. Munzar, T. Aoki, S.O. Kasap, J. Mater. Sci.: Mater. Electron, **18**, 000 (2007) [in press].
[22] S. O. Kasap, K. Koughia, M. Munzar, D. Tonchev, D. Saitou T. Aoki, J. Non-Cryst. Solids, **353** 1364 (2007).
[23] M. Needls, M. Schlüter, M. Lannoo, Phys. Rev. B **47**, 15533 (1993).

*Corresponding author: aoki@ee.t-kougei.ac.jp